Abstract

This doucument describes the quantum trajectories method of quantum Monte-Carlo simulation, which I then implement in a laser cooling code using the Armadillo C++ library for complex matrix manipulation. I first demonstrate that the code replicates results from a simple J=0→J'=1 transition (specifically, I test reproduction of Rabi Oscillations and of Force v Velocity). Next, I show that the code accurately reproduces the features of polarization gradient cooling in 1D J=1→J'=2 AND J=1→J'=1 schemes (the latter of which should have an 'anti-damping' force for red detuning at low velocities). Next, I demonstrate the effect of Λ-enhanced cooling for a simple system with two ground states (J=3/2 and J=1/2) and one excited state (J=1/2). Finally, I test 3D simulations of the quantum trajectories code for J=1 to J'=1 (for comparison to [3]) and of our own system, both with 1 beam (testing if we can really cool to 5μK with just 1 laser, as Mike Tarbutt claims) and with a Λ scheme.

Laser Cooling: Quantum Trajectories Model and Implementation

Thomas Langin

July 29, 2022

0.1 What is the "Quantum Trajectories" method, and how can we get laser-forces from this?

Quantum trajectories is a technique for simulating how particle-light coupling can induce an evolution of the wavefunction of a particle and the resulting atom-light forces. Applied over a large enough number of particles, the results should be identical to an optical bloch equation (OBE) solution. However, quantum trajectories has a number of advantages over an OBE solver: for one, it can be integrated in an N body simulation that includes inter-particle forces (though this is not so important for an ultracold molecule application). Another advantage is that it directly accounts for the effects of spontaneous emission, while OBE solvers must rely on a model for the 'random-walk' heating (I can imagine this being particularly important for accurate simulations of Λ enhanced cooling, since the discretized nature of the kicks may have a non-trivial effect on the likelihood for atoms to become 'trapped' in the VSCPT state compared to a 'continuous heating' model). Finally, for simulations over a very large Hilbert space (N states), less information is required to store the particle wavefunctions ($2N$ numbers per molecule) than would be for storing density matrices ($2N^2$).

The equivalence between QT and the OBE/Master Eq approach was demonstrated separately by two groups: Dalibard, Castin, and Molmer [4] and Carmichael [5], and explained clearly in Chapter 6 of M. Lukin's textbook on Atomic physics [1]; my introduction here will largely follow the approach in Lukin. The basic approach is to identify an equivalence between the master equation, which describes the time evolution of a density matrix ρ_s in an open quantum system, and the evolution of a wavefunction $|\psi\rangle$ under a *non-Hermitian* Hamiltonian which can also, during any timestep, 'jump' via spontaneous emission to 'ground states' $|g\rangle$ with a probability determined by the current expectation value for the 'excited state' population $|\langle e|\psi\rangle|^2$.

The master equation for the evolution of a pure quantum state, in its most general form, can be written

$$\frac{d\rho_s}{dt} = \frac{1}{i\hbar}\left[H_s, \rho_s\right] - \sum_k \frac{\gamma_k}{2}\left(c_k^\dagger c_k \rho_s + \rho_s c_k^\dagger c_k - 2c_k \rho_s c_k^\dagger\right) \tag{1}$$

where c_k are "decay jump" operators with associated rate γ_k (e.g. $c_1 = |1\rangle\langle 2|$ implies that atoms in state $|2\rangle$ decay to $|1\rangle$ at a rate γ_1), and H_s is the "system Hamiltonian", which is independent of coupling to the reservoir/vacuum. The second term on the RHS of Eq. 1 is often referred to as the 'Liouvillian' operator. By simple grouping of terms, Eq. 1 can be rewritten as

$$\begin{aligned}\frac{d\rho_s}{dt} &= \frac{1}{i\hbar}\left(H_{eff}|\psi\rangle\langle\psi| - |\psi\rangle\langle\psi|H_{eff}^\dagger\right) + \sum_k \gamma_k c_k |\psi\rangle\langle\psi| c_k^\dagger \\ &= \frac{1}{i\hbar}\left[H_{eff}, \rho_s\right] + \sum_k \gamma_k c_k |\psi\rangle\langle\psi| c_k^\dagger\end{aligned} \tag{2}$$

where $|\psi\rangle\langle\psi| = \rho_s$ and $H_{eff} = H_s - i\hbar\sum_k \frac{\gamma_k}{2} c_k^\dagger c_k$.

The first term on the RHS corresponds to the evolution of a pure state $|\psi\rangle$ under the *non-Hermitian* Hamiltonian H_{eff}, i.e.

$$i\hbar\frac{d}{dt}|\psi\rangle = H_{eff}|\psi\rangle. \tag{3}$$

According to this Hamiltonian, if we start with a wavefunction $|\psi(t)\rangle$ at time t, then at time $t+dt$ the wavefunction is written as

$$|\psi(t+dt)\rangle_{wrong} = \left(1 + \frac{H_{eff}\delta t}{i\hbar}\right)|\psi(t)\rangle \tag{4}$$

The reason I added the "wrong" subscript is because it turns out that this wavefunction is *not normalized* due to the non-Hermitian nature of H_{eff}. Assuming that $|\psi(t)\rangle$ is normalized, it turns out that ${}_{wrong}\langle\psi(t+dt)|\psi(t+dt)\rangle_{wrong} = 1 - dt\sum_k \gamma_k\langle\psi(t)|c_k^\dagger c_k|\psi(t)\rangle = 1 - dp$, where we've defined

$$dp = dt\sum_k \gamma_k\langle\psi(t)|c_k^\dagger c_k|\psi(t)\rangle = \sum_k dp_k \tag{5}$$

where, as we'll see later, dp is the probability that the wavefunction has "jumped". So, to get the normalization right, we define:

$$|\psi(t+dt)\rangle_{correct} = \frac{1 + H_{eff}dt/i\hbar}{\sqrt{1-dp}}|\psi(t)\rangle \tag{6}$$

where, in the rest of this chapter, I'll drop the "correct" subscript.

The second term on the RHS of Eq. 2 handles quantum jumps that change $|\psi\rangle$ into another state $|\phi_k\rangle = c_k|\psi\rangle$, which are caused by the coupling to the external environment that results in, for example, spontaneous emission. However, we can see that these states are also unnormalized, since $\langle\phi_{k,wrong}|\phi_{k,wrong}\rangle = \langle\psi|c_k^\dagger c_k|\psi\rangle = dp_k/(\gamma_k dt)$. Thus, we can define the proper normalized state $|\phi\rangle_{k,correct} = \sqrt{\gamma_k dt/dp_k}|\phi_{k,wrong}\rangle$. In the rest of the chapter, I'll drop the "correct" subscript.

The master equation in Eq. 2 can be propagated for discrete time dt, yielding

$$\begin{aligned}\rho_s(t+dt) &= |\psi(t+dt)\rangle_{wrong\ \ wrong}\langle\psi(t+dt)| + dt\sum_k \gamma_k|\phi_k\rangle_{wrong\ \ wrong}\langle\phi_k| \\ &= (1-dp)|\psi(t+dt)\rangle\langle\psi(t+dt)| + \sum_k dp_k|\phi_k\rangle\langle\phi_k|.\end{aligned} \tag{7}$$

This equation can be interpreted in the following way: given a wavefunction $|\psi(t)\rangle$, in a timestep dt the wavefunction will either evolve to $|\psi(t+dt)\rangle$ according to Eq. 6 with probability 1-dp or, with probability dp_k, the wavefunction will jump into one of the $|\phi\rangle_k$ states. This is relatively straightforward to implement in a computer simulation through the following algorithm:

- Pick initial state $|\psi(0)\rangle$
- Pick random number r

- Calculate dp over some interval dt. If $dp < r$, $|\psi\rangle$ evolves according to Eq. 6. If $dp > r$, jump to $|\phi\rangle_k$ with probability determined by dp_k/dp (this will involve 'rolling' another random number) (NOTE: change this to reflect new jump technique)
- Repeat steps (2) and (3) over as many particles as you want for as many timesteps as you want.

To calculate forces, one simply takes the expectation value of the force, which can be calculated in the Heisenberg picture:

$$\langle F \rangle = -\langle [\nabla, H] \rangle \approx -\langle -\nabla H_{eff} \rangle \tag{8}$$

where in the last step we assume that the user-defined basis sets are not changing in space (this is typically true for most QT simulation: one sticks with the same basis (e.g. $|J, J_z\rangle$) at all points).

0.2 Implementation of spatially dependent light fields

We can clearly see from Eq. 8 that, if H_{eff} varies in space, the particle will experience a force as it moves through the light field. For a simple example, consider the case of two counter-propagating, oppositely circularly polarized, lasers exciting a $J = 0$ to $J' = 1$ transition. The Electric field can be written as

$$\vec{E}(z,t) = \frac{E_0}{\sqrt{2}} \exp\left(-i\omega_L t\right) \left[\left(-\hat{x} - i\hat{y}\right) e^{ikz} + \left(\hat{x} - i\hat{y}\right) e^{-ikz}\right] + c.c \tag{9}$$

where E_0 is the electric field amplitude, ω_L is the laser frequency, k is the laser wavelength, and z is the axis of laser propagation. This can be simplified to

$$\vec{E}(z,t) = -\sqrt{2} E_0 i \exp\left(-i\omega_L t\right) \left[\hat{x}\sin(kz) + \hat{y}\cos(kz)\right] + c.c \tag{10}$$

When considering the atom-light coupling, we are primarily concerned with how the light field couples different electronic states. The 'portion' of light that is $\sigma^+ = (-\hat{x} - i\hat{y})/\sqrt{2}$ (here we are considering the m_z basis) is available to excite $m \to m+1$ transitions, the $\sigma^- = (\hat{x} - i\hat{y})/\sqrt{2}$ portion excites $m \to m-1$ transitions. Thus, we calculate:

$$c'_{\sigma^+} = \langle \vec{E} \cdot \sigma^+ \rangle = E_0 \exp\left(-i\omega_L t\right) \left[i\sin(kz) + \cos(kz)\right] \tag{11}$$

and

$$c'_{\sigma^-} = \langle \vec{E} \cdot \sigma^- \rangle = E_0 \exp\left(-i\omega_L t\right) \left[-i\sin(kz) + \cos(kz)\right] \tag{12}$$

To simplify the picture, we move into a frame rotating at a frequency $\omega_L a$, and define $\Omega - dE_0/\hbar$, where d is dipole moment for the transition, and rewrite the 'primed components' above as:

$$c_{\sigma^+} = i\sin(kz) + \cos(kz) \tag{13}$$

and

$$c_{\sigma^-} = -i\sin(kz) + \cos(kz) \tag{14}$$

In this approximation, we ultimately arrive at the below 'atom-light' hamiltonian for the $J = 0 \rightarrow J' = 1$ transition:

$$H_{AL} = \frac{\hbar\Omega}{2} c_{\sigma^+}(z)|e+\rangle\langle g| + \frac{\hbar\Omega}{2} c_{\sigma^-}(z)|e-\rangle\langle g| - \hbar\delta\left(|e-\rangle\langle e-| + |e+\rangle\langle e+|\right) \tag{15}$$

where $|e+\rangle$ refers to the $|J' = 1, m_j = +1\rangle$ state, $|e-\rangle$ refers to the $|J' = 1, m_j = +1\rangle$ state, and $\delta = \omega_L - \omega$ where ω is the energy of the excited state (here we set the ground state to zero energy).

Taking the derivative with respect to z, we find:

$$\langle F\rangle = -\langle\frac{dH}{dz}\rangle = \hbar k\Omega\left[\cos(kz)\left(-Im(\rho_{ge-}) + Im(\rho_{ge+})\right) + \sin(kz)\left(Re(\rho_{ge-}) + Re(\rho_{ge+})\right)\right] \tag{16}$$

where $\rho_{ab} = \langle\psi|b\rangle\langle a|\psi\rangle$ and $\psi\rangle$ is the particle's wavefunction. If we want, we can then add a step to the list of steps beginning on page 2 where we update the particle's 'velocity' according to the force. Or else we can just hold 'v' constant while determining the force averaged over some sufficiently long period of time to obtain $F(v)$, the force as a function of a particle's velocity.

Here I'll just note that typically these sort of simulations are preformed using 'natural' units (times and frequencies normalized by Γ, the spontaneous emission rate from some excited state, position normalized by k, velocity normalized by k/Γ, energy by $\hbar\gamma$, etc.). This makes the simulation much more generalizable and removes the difficulty from considering 'small' units like nm and large units like $10^8 \mathrm{s}^{-1}$, a typical value for Γ.

0.3 Test 1: J=0→J'=1

I first applied the code to the 'simple' case of a $J = 0$ to $J' = 1$ transition driven by counter-propagating circularly polarized beams propagating along z. For the first test of the code, I compare the evolution of $\langle p_{--}(t)\rangle$, $\langle p_{++}(t)\rangle$, $\langle p_{gg}(t)\rangle$, and $F(v,t)$ from the QT code (here $\langle\rangle$ represent ensemble averages over the number of particles in the QT simulation, $p_{--} = \langle\psi|e-\rangle$, etc.) to an exact solution from the simple OBEs for this system, reproduced below:

$$\frac{d\rho}{dt} = \left[-\frac{\Gamma}{2}\left[\left(|e+\rangle\langle e+| + |e-\rangle\langle e-|\right)\rho + \left(p_{++} + p_{--}\right)|g\rangle\langle g|\right] + h.c.\right] + \frac{1}{i\hbar}\left[H_{AL}, \rho\right] \tag{17}$$

where, in this case, H_{AL} is given by

$$H_{AL} = (-\delta + kv)|e-\rangle\langle e-| + (-\delta - kv)|e+\rangle\langle e+| - \frac{\hbar\Omega}{2}\left(|g\rangle\langle e+| + |g\rangle\langle e-|\right) \quad (18)$$

We should, of course, see damped Rabi oscillations along with a non-zero force for $v \neq 0$. We test the QT code for two scenarios (both of which have $\Omega = \Gamma$ and $\delta = -\Gamma$): $kv/\Gamma = 0$ and $kv/\Gamma = 0.5$. The results of both the QT and the OBE solver are shown below: clearly we have demonstrated good agreement.

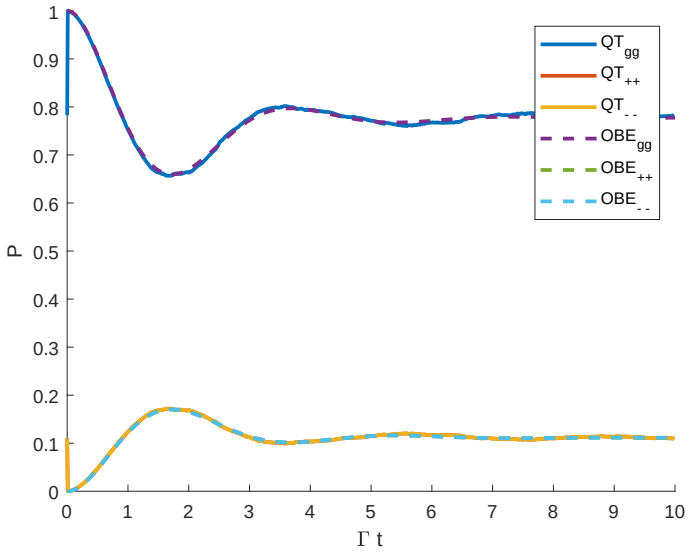

Figure 1: Rabi oscillations for $v = 0$, $\Omega = \Gamma$ and $\delta = -\Gamma$, determined both from the OBE solutions (dashed lines) and the QT simulation (solid lines), for a 3 level system. We see good agreement between QT and OBEs.

The next test is to determine whether $F(v)$ from the QT simulation matches the OBE solver. We calculate $F(v)$ by averaging the force on each particle calculated during each step of the QT simulation over all particles and over all time. Each simulation contains 10 particles all moving with velocity v, with independently evolving wavefunctions (e.g., jumps are un-correlated). The results from the QT show good agreement with the OBE solver (Fig. 4).

0.4 Test 2: J=1→J'=2

Next, we move on to something a little less trivial: a $J = 1$ to $J' = 2$ system. It is possible to generate sub-Doppler forces in this configuration by using a so-called $\pi_x - \pi_\phi$ scheme, due to polarization gradients [6]. In such a scheme, one sets up counter-propagating linearly polarized lasers, with an angle ϕ between the polarization axes (one laser is always assumed to be polarized along x). The field then becomes:

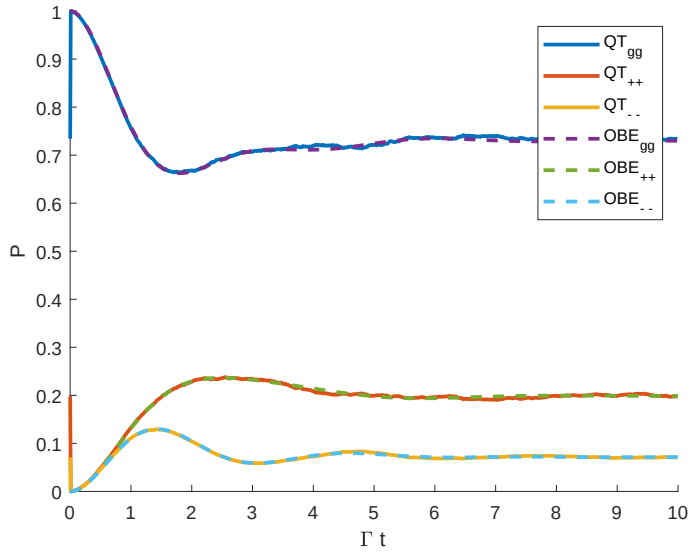

Figure 2: Same as Fig. 1 except kv/Γ=0.5. Agreement is still good.

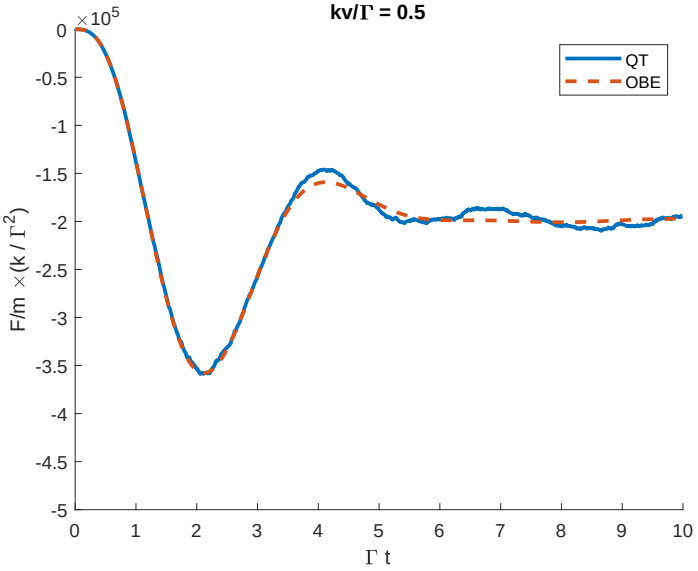

Figure 3: Force vs time for the $kv/\Gamma = 0.5$ case. Agreement is good.

$$\vec{E}(z,t) = E_0 \exp\left(-i\omega_L t\right)\left[\hat{x}e^{ikz} + \left(\cos(\phi)\hat{x} + \sin(\phi)\hat{y}\right)e^{-ikz}\right] + c.c \qquad (19)$$

One can then (eventually) derive c_{σ^+} and c_{σ^-} in the same way as above to find:

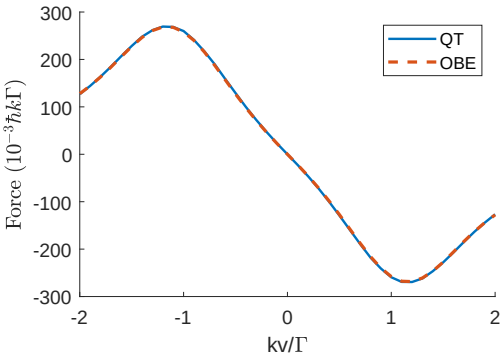

Figure 4: Force (after steady-state is achieved) vs velocity for $\Omega = \Gamma$, $\delta = -\Gamma$ and $kv/\Gamma = 0.5$. We see good agreement between the QT and OBE simulation.

$$c_{\sigma^+} = \frac{1}{\sqrt{2}}\left[\cos(kz) \times (-1 - \cos(\phi) + i\sin(\phi)) + \sin(kz) \times (-i + i\cos(\phi) + \sin(\phi))\right] \tag{20}$$

and

$$c_{\sigma^-} = \frac{1}{\sqrt{2}}\left[\cos(kz) \times (1 + \cos(\phi) + i\sin(\phi)) + \sin(kz) \times (i - i\cos(\phi) + \sin(\phi))\right] \tag{21}$$

The force is then calculated from the resulting H_{AL} as before (NOTE: Now that we are working with a transition with non-unity 3j symbols, we must make sure to correctly account for those (e.g.: while $|m = -1\rangle \rightarrow |m' = -2\rangle$ 3j symbol is unity, the $|m = 0\rangle \rightarrow |m' = -1\rangle$ symbol is $\sqrt{\frac{1}{2}}$, thus the coupling term for that transition becomes $c_{\sigma^-}(z)\hbar\Omega/\sqrt{2}|m' = -1\rangle\langle m = 0|$, etc. This will also affect the 'jump' probabilities. The QT code takes all of this into account).

We will use the results presented in [3] as a point of comparison. The top row of Figure 1 from that paper (reproduced below as Fig. 5) shows the $F(v)$ curve for this scheme (which they call linϕlin) derived using their OBE solver. (NOTE: the second row covers $J = 1 \rightarrow J' = 1$, the subject of the next chapter) for $\Omega = \Gamma/\sqrt{2}$ and $\delta = -2.5\Gamma$. The 'high velocity' data demonstrates 'typical' Doppler cooling while the 'low velocity' data shows the sub-Doppler 'polarization gradient' cooling [6].

The results from the 'first' QT attempt are shown below (Figs. 6- 10). For this attempt, we use 10 particles, all starting at $z = 0$. We observe that, for $\phi = \pi/2$, we observe both Doppler-cooling AND polarization gradient sub-doppler cooling, as expected, while for $\phi = 0$ we MOSTLY observe Doppler cooling without the sub-Doppler component. However, we do observe a seemingly interesting pattern at low velocities, where we appear to observe sub-doppler HEATING (green curve in Fig. 7). This, however, is an artifact from starting all of the atoms at the same position. In this case, for 'low' velocities, the

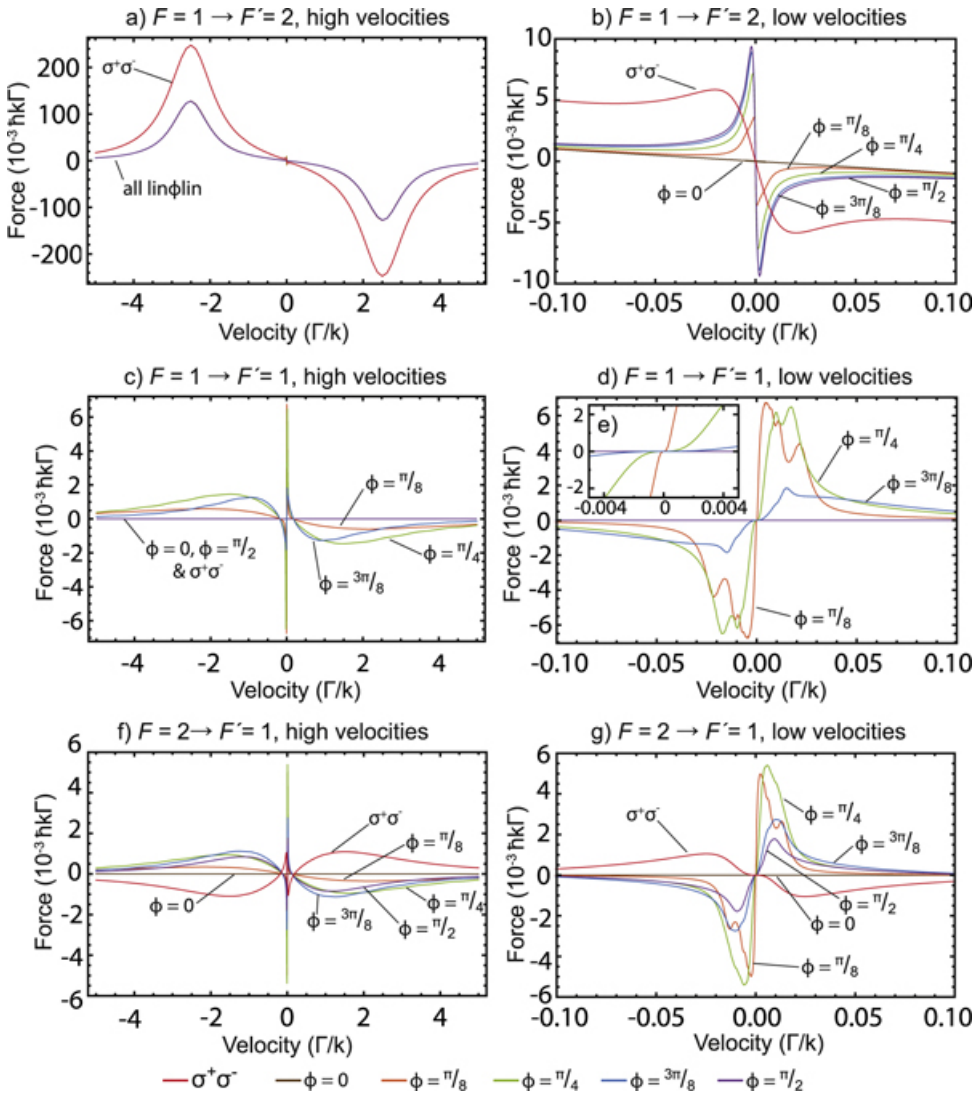

Figure 5: Results from [3]. These are from OBE simulations of various systems with 1D cooling with $\Delta = -2.5\Gamma$ and $\Omega = \Gamma/\sqrt{2}$. In the top row we have a $F = 1$ to $F' = 2$ transition, which should exhibit doppler cooling and, under appropriate polarization schemes, sub Doppler polarization-gradient cooling. In the middle row we have a $F = 1$ to $F' = 1$ transition, for which we expect only sub-doppler polarization gradient HEATING, and only for $\phi \neq 0,\pi/2$.

$F(t)$ graph averaged over all of the particles is sinusoidal (red curve in Fig. 8). For certain velocities, this will lead to a non-integer number of cycles being completed (red curve in Fig. 8); in the event that this occurs, there will be a non-zero force when averaging over all time. This is what we are observing. If the positions were randomized, the phase of the $F(t)$ graph for each particle would be different and the force will average to zero (blue curve in Fig. 8). I re-ran the simulation with 100 particles with random positions: in this case, we

observe zero force at low v, as expected (blue curve in Fig. 7).

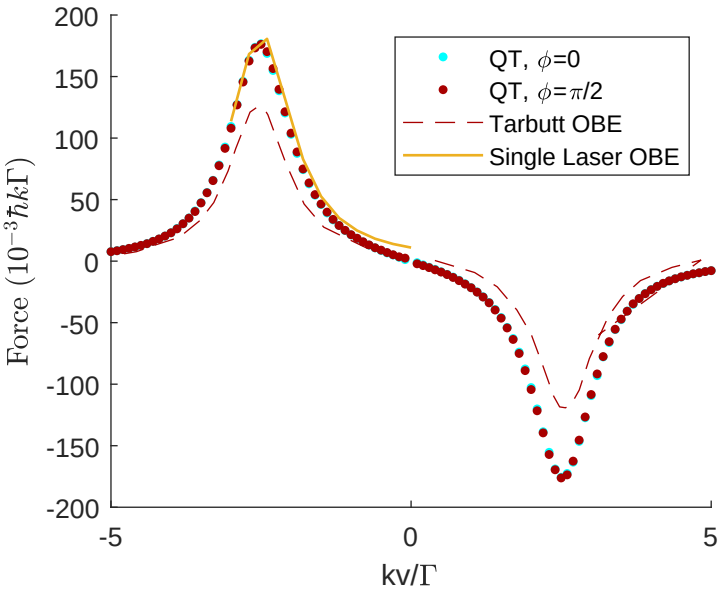

Figure 6: Comparison between my QT results (points) and the Tabutt OBE results (dashed) from top row of Fig. 5 for $F(v)$ 'high velocities'. Here we see the expected Doppler cooling. My results do seem to differ from the Tarbutt results, but agree largely with a single laser OBE code (e.g., only include the rightward propagating laser) in the v¡¡0 regime, which makes me think that Tarbutt used a slightly lower value for Ω than was reported.

Here I will point out that the forces we observed are a little bit higher than the forces observed by Tarbutt, both for Doppler and sub-Doppler cooling. However, I think that my results are accurate: For $kv \sim -\delta$, we expect the atoms to be almost exclusively absorbing light from one of the beams. For a single beam, it is pretty easy to solve the OBEs: This is demonstrated in the yellow curve of Fig 9 The solution clearly agrees with my QT simulation more than the Tarbutt OBE solver (my guess is they just defined Ω slightly differently and didn't indicate this in their paper...)

0.5 Test 3: J=1→J'=1

Now, we move on to a $J = 1 \rightarrow J' = 1$ system. Naively, one would expect no-cooling for such a system. To see this, consider each laser independently. The particle has at least one state that is dark for each beam (for circularly polarized light this is obvious: a particle in $m = +1$ cannot absorb from a σ^+ laser operating on a J=1 to J'=1 transition. For linearly polarized light, we must consider the fact that a $m = 0$ to $m' = 0$ transition has a clebsch-gordon coefficient of zero.). If the particle 'wants to' absorb from a given beam (e.g., the beam it is moving towards) it will do so until it decays into the state dark

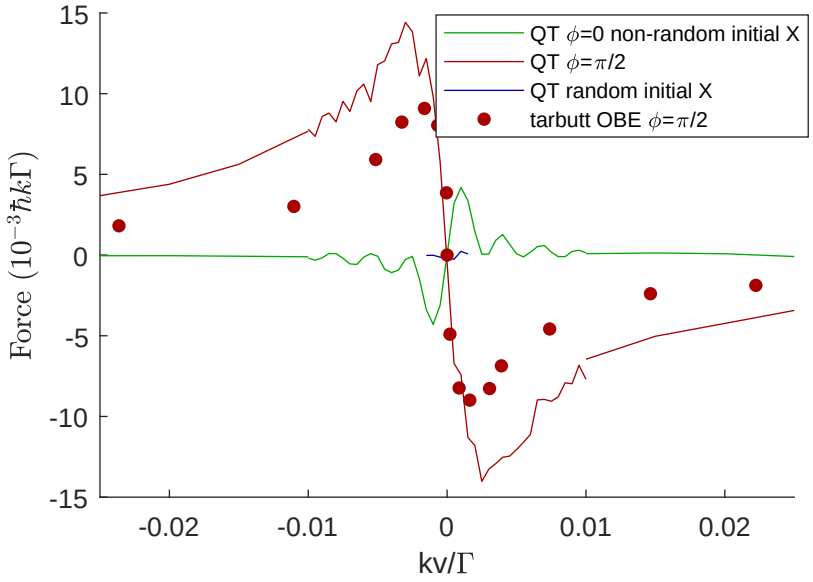

Figure 7: $F(v)$ for low velocities, again comparing my QT results to the Tarbutt OBE results. We again see good qualitative agreement (in the $\pi/2$ case), with my force (red line) appearing to be slightly higher. The $\phi = 0$ results with non-random initial position (green) seems to show some subDoppler heating, however, this is just a consequence of the non-random initial position and the finite simulation time (see Fig. 11). When positions are randomized, this force is negligible, as expected (blue)

to that beam, at which point it is stuck until it absorbs from the 'wrong' beam. Thus, we see that the particle cannot 'cycle' photons from the 'correct' beam, but will instead absorb equally from each beam, leading to a net force of zero.

However, the picture is a little bit different for the case of counter-propagating linearly polarized beams for an atom moving with $v \ll \Gamma/k$. In this limit, there is a Sisyphus mechanism that delivers a net force, similar to the case in a Type I transition. Consider $\phi = \pi/4$. In this case, we have an intensity gradient and a polarization gradient, a positionally dependent dark state (as in, the quantum state that is dark to the light field depends on the particle's position) and bright states. At intensity maxima, an atom in the bright state is most likely to be pumped down to the dark state. As the now dark atom moves through the light field, it can make a non-adiabatic transition into a bright state (the motion of the atom changes what state is 'dark', so there is a non-zero inner product between the dark state at time t and the bright state at time $t + dt$, over which the atom has moved by vdt). The transition is most likely to occur when the atom is at an intensity minimum (the two states are closest in energy due to this being the location of the weakest AC stark shift). This bright atom then falls down the AC stark potential (for RED detuning) towards high intensity, where it is most likely to be pumped to the dark state, and so on. The atom thus GAINS energy for red detuning whenever it is in the bright state. So, we expect to see sub-Doppler HEATING for red detuning in a Type II atom, the

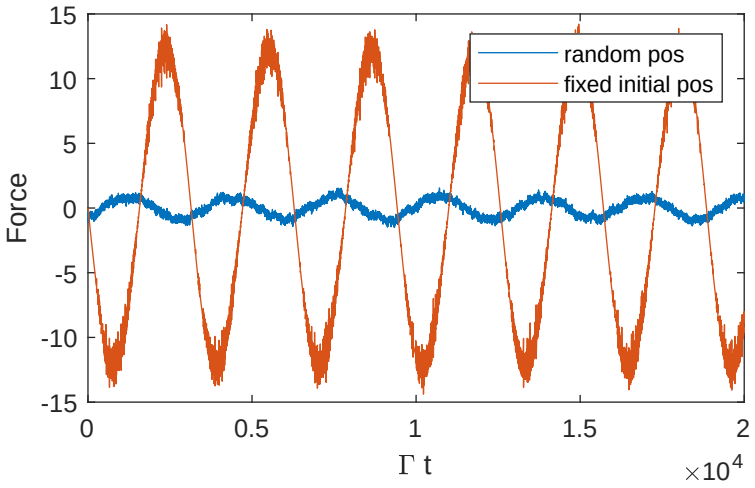

Figure 8: Force vs Time for kv/Γ =???? with random and non-random initial positions. We see that the force is periodic; simulating for a non-integer number of oscillation periods will lead to a the observation of a 'force'. Upon randomizing the positions, the force disappears; this is because now each particle's F vs t curve has a different phase.

opposite of what we expect for Type I (see middle row of Fig. 5)

This force does not exist for $\phi = 0$ due to the fact that there is no polarization gradient: the atom will just get trapped in a dark state and never escape. It also doesn't exist for $\phi = \pi/2$ because in this case there is no intensity gradient, and thus the AC stark shift for the bright state does not change with the atom position. In other words, we need both a polarization gradient AND an intensity gradient for any sub-Doppler forces in a type II system irradiated by counter-propagating 1D beams.

We indeed see this in our QT code. For high velocity, the forces are negligible (see Fig. 9). For low velocity, we see a strong heating force for $\phi = \pi/4$, and no force for $\phi = 0$ or $\phi = \pi/2$ (Fig. 10). Also, we observe that, for the case when all particles start with the same initial position, the force vs time plot is periodic as it is for a Type I system (Fig. 11). The functional form is a little bit more complicated, however.

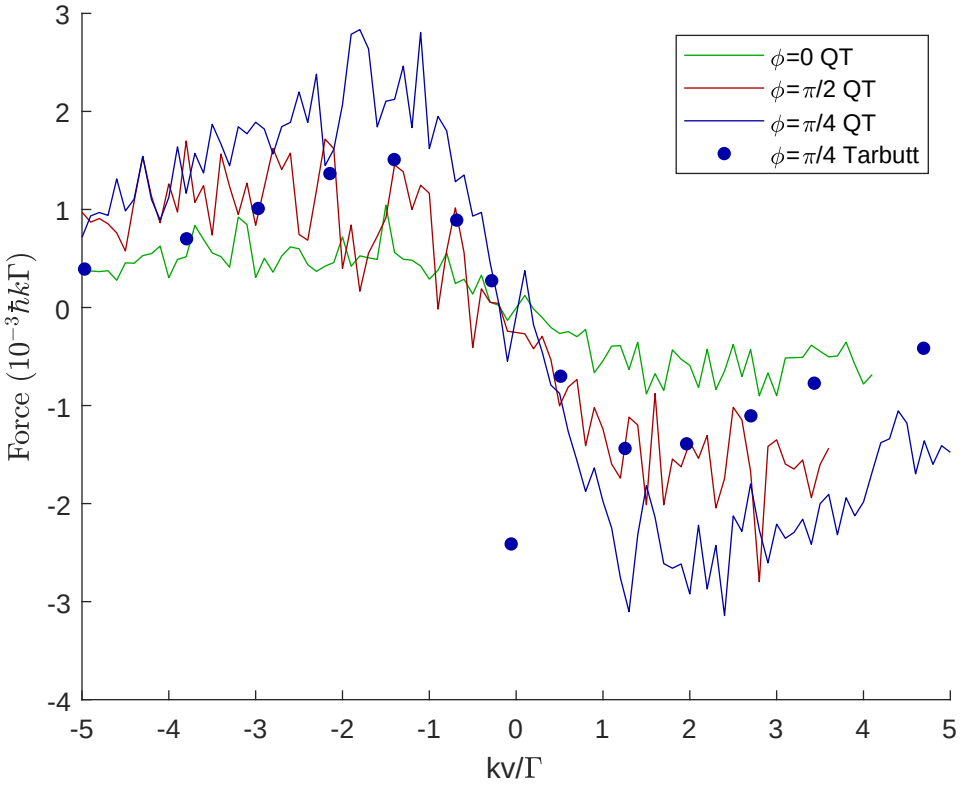

Figure 9: High vel results for $J = 1$ to $J' = 1$ cooling scheme. We observe very little in the way of doppler cooling, as expected.

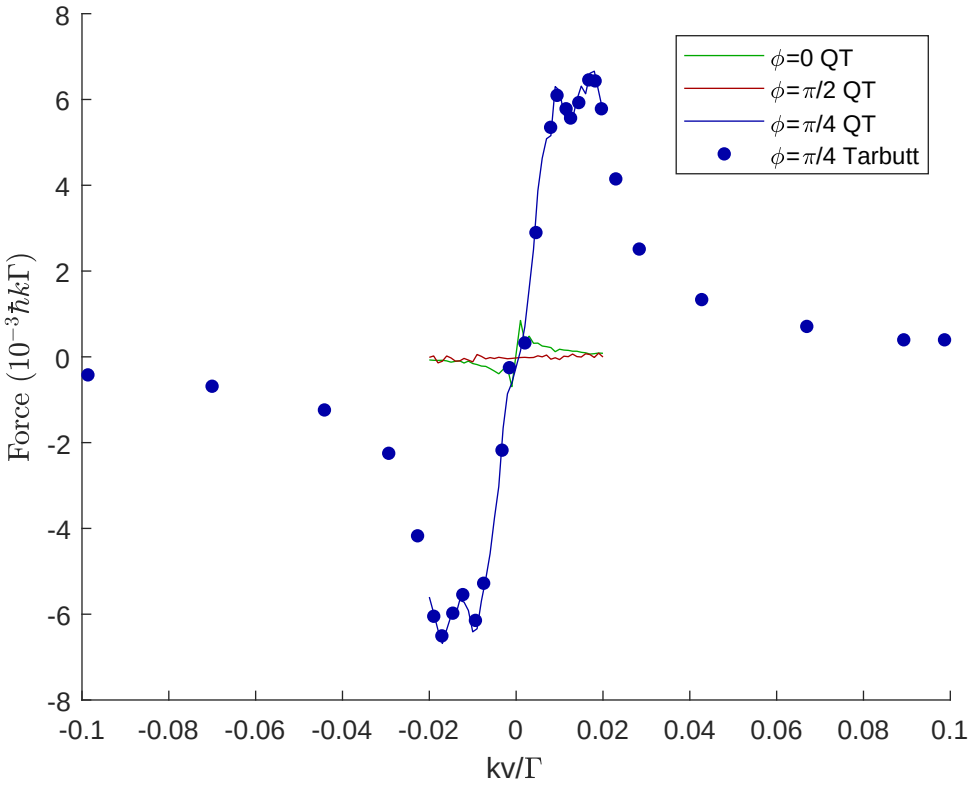

Figure 10: Low vel results for varous ϕ for $J = 1$ to $J' = 1$ cooling. We observe a substantial force for $\phi = \pi/4$. The force is negligible for any other ϕ. Our results agree with the results from the Tarbutt group [3].

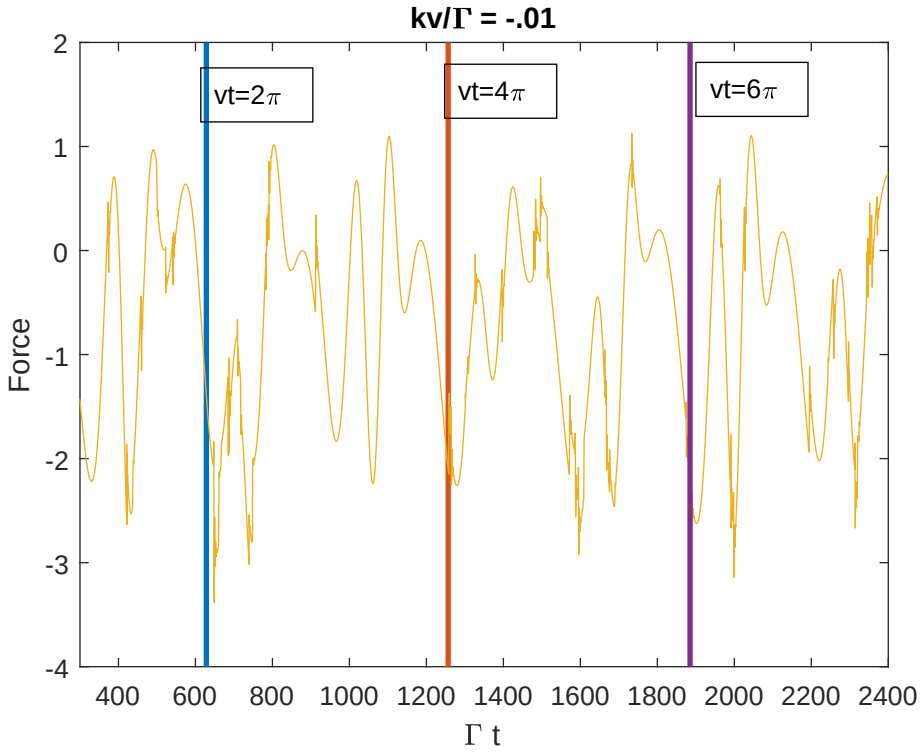

Figure 11: $F(t)$ for $\phi = \pi/4$ and $kv/\Gamma = -0.01$ where all particles start with $x = 0$. We observe that the force is periodic $T = 2\pi/v$, as expected, and is clearly 'net-negative'.

Chapter 1

Three Dimensional Cooling

The next step in developing a QT code for 3D cooling of SrF is to, well, make the code 3D. Here we will consider 3 orthogonal pairs of counter-propagating lasers in the σ^+-σ^- configuration, as is the case in our SrF MOT. The electric field is given by:

$$\vec{E} = -\sqrt{2}E_0 i \left[\hat{x}\left(\sin kz + \cos ky\right) + \hat{y}\left(\sin kx + \cos kz\right) + \hat{z}\left(\sin ky + \cos kz\right)\right] \tag{1.1}$$

and we have:

$$c_{\sigma^+} = i\left[\sin kz + \cos ky\right] + \left[\cos kz + \sin kx\right], \tag{1.2}$$

$$c_{\sigma^-} = -i\left[\sin kz + \cos ky\right] + \left[\cos kz + \sin kx\right], \tag{1.3}$$

and

$$c_{\pi} = -\sqrt{2}i\left[\sin ky + \cos kx\right] \tag{1.4}$$

Now consider a system with one excited state and one ground state, each of which has a Zeeman substructure. In this case, we can in general write the 'coupling' part of the Hamiltonian (i.e., all the terms with a 'Rabi Frequency') as:

$$\begin{aligned} H_{coup} = \frac{\hbar\Omega}{2}\Big[& c_{\sigma^+}\gamma_{m,m+1,J,J'}\sum_m |e,m+1\rangle\langle g,m| \\ & + c_{\pi}\gamma_{m,m,J,J'}\sum_m |e,m\rangle\langle g,m| \\ & + c_{\sigma^-}\gamma_{m,m-1,J,J'}\sum_m |e,m-1\rangle\langle g,m|\Big] \end{aligned} \tag{1.5}$$

where $\gamma_{m,n,J,J'}$ refers to the dipole matrix element coupling the two states (typically given by $\gamma_{m,n,J,J'} = \Gamma w_{m,n,J,J'}$), where $w_{m,n,J,J'} \leq 1$ is typically some product of Wigner 3j and 6j symbols and other prefactors depending on J and J' (here J and J' do not necessarily refer to the total angular momentum, but rather stand in as a placeholder for ALL relevant quantum numbers...of which

there are many for SrF). Later I will walk through a calculation of the w values for the relevant SrF transitions (it's not worth the space to demonstrate a calculation of these values for standard atomic $F \rightarrow F'$ transitions...these can be easily looked up, as can the values for ^{6}Li, which I use to test a Λ cooling scheme in Sec. 1.2). The force is, again, simply given by Eq. 8.

The QT evolution algorithm is the same as in the 1D case, the only difference now is that the the values of $c_{\sigma_+,\sigma_-,\pi}$ depend on x, y, and z, not just z, and the force is thus also 3D in nature. The 3D system contains polarization and intensity gradients, and therefore we might expect that the sub-Doppler heating observed for red-detuning in a Type II system in the special case of $\phi = \pi/4$ will now apply to a 3D $\sigma^+ - \sigma^-$ system (no heating or cooling is observed in 1D $\sigma^+ - \sigma^-$ configuration for a Type II system!).

1.1 3D Tarbutt Comparisons

Cooling and heating in a 3D configuration was also examined by the Tarbutt group [3] for a $F = 1 \rightarrow F' = 1$ transition. First, they examined the force along one axis (x) as a function of v_x while v_y was set to 0 and v_z was set to 0.1 (NOTE: unless otherwise stated, all velocities are in units Γ/k from here on out). I did the same thing with my QT code. I also examined forces along other axes (F_y vs. v_y with $v_z = 0$ and $v_x = 0.1$ and F_z vs v_z with $v_x = 0$ and $v_y = 0.1$). In Fig. 1.1, I compare the QT results to the Tarbutt group results. Good qualitative agreement is observed, although for $v > 1$ the simulations do disagree a bit from the Tarbutt group results. My guess is that I tried to use too large of a timestep (the timestep that one uses should shrink with velocity). In any case, ultimately this code will be primarily concerned with $v \ll 1$ (for reference: for SrF at 50μK, $\langle v_{rms} \rangle = 0.0142$.), so I am satisfied with the observed agreement.

Next, the Tarbutt group considered a generalized 'force vs speed' graph, where they plot $\vec{F} \cdot \vec{v}/|v|$ for various v, where F is averaged over 500-5000 random trajectories for a given choice of $|v|$. I was a little lazy here, so I 'only' used 25 random trajectories to test my QT code against the Tarbutt results. In Fig. 1.2 I compare the QT results to the Tarbutt OBE's for various dt. For low dt we see good agreement throughout the velocity range considered, however, as dt increases, the curves begin to diverge at high speed (basically, for an accurate simulation, you need $vdt \ll \lambda$).

1.2 Λ cooling, J=3/2 and J=1/2 to J'=1/2

Our ultimate goal is to simulate 3D Λ enhanced cooling of SrF. First, a quick review on Λ enhanced cooling:

1.3 SrF Cooling

First, let's introduce the level diagram. (insert level diagram).

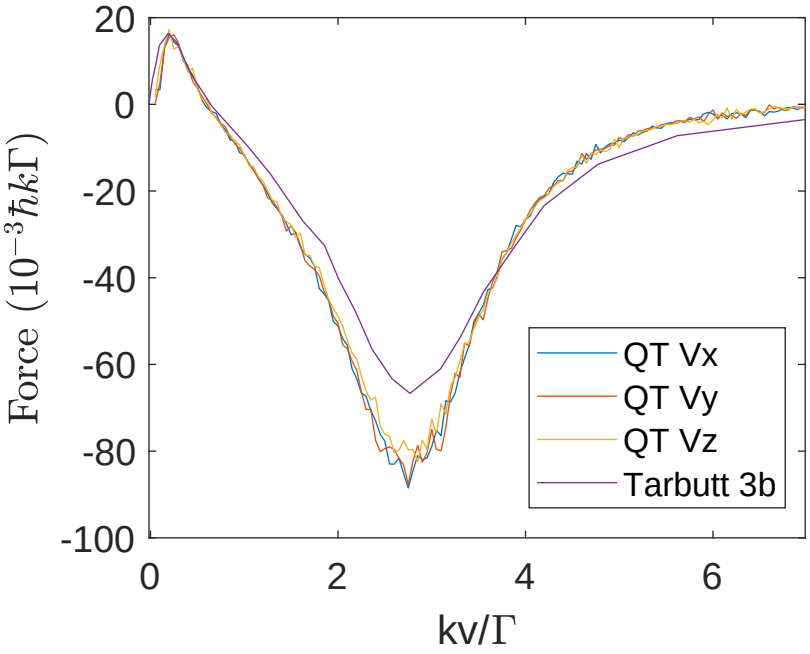

Figure 1.1: F vs v along some axis where the velocities along the other two axes are set to 0 and 0.1 ($\delta = -2.5$, $\Omega = 1$). We observe good qualitative agreement between the QT simulation and the Tarbutt group results throughout, along with good quantitative agreement for $v < 1$. At higher v, we observe some disagreement; this is possible because I set the timestep to be too large (0.04), see Fig. 1.2

.

Normally, the next step would be to go calculate all of the relevant CG coefficients (e.g., from F=2 to F'=1,0, F=1 to F'=1,0, etc.). For molecules, the story is a little more complicated. First, X and A, the two electronic states, are expressed in two different "Hunds cases" (B and A respectively). A is appropriate when the spin-orbit term ($H_{SO} = A\vec{L}\cdot\vec{S}$) is larger than any rotational or HFS or spin rotation splitting, while B is appropriate when H_{SO} is negligible. On top of this, two of the X states ($|F = 1\uparrow\rangle$ and $|F = 1\downarrow\rangle$) are actually combinations of J states ($|F = 1\uparrow\rangle = 0.888|J = 3/2\rangle + 0.4598|J = 1/2\rangle$ and $|F = 1\downarrow\rangle = -0.4598|J = 3/2\rangle + 0.888|J = 1/2\rangle$).

We follow the following steps to obtain the CG coefficients:

- express all X states as sums of pure J states.
- rewrite all X states in the (a) basis (they will thus be sums of pure J and pure Ω states, as Ω is a good quantum number only in (a))
- write the A states (positive parity) in terms of basis states of signed Ω using Eq 6.234 of Brown and Carrington
- use angular momentum summation rules to determine CGs based on inner

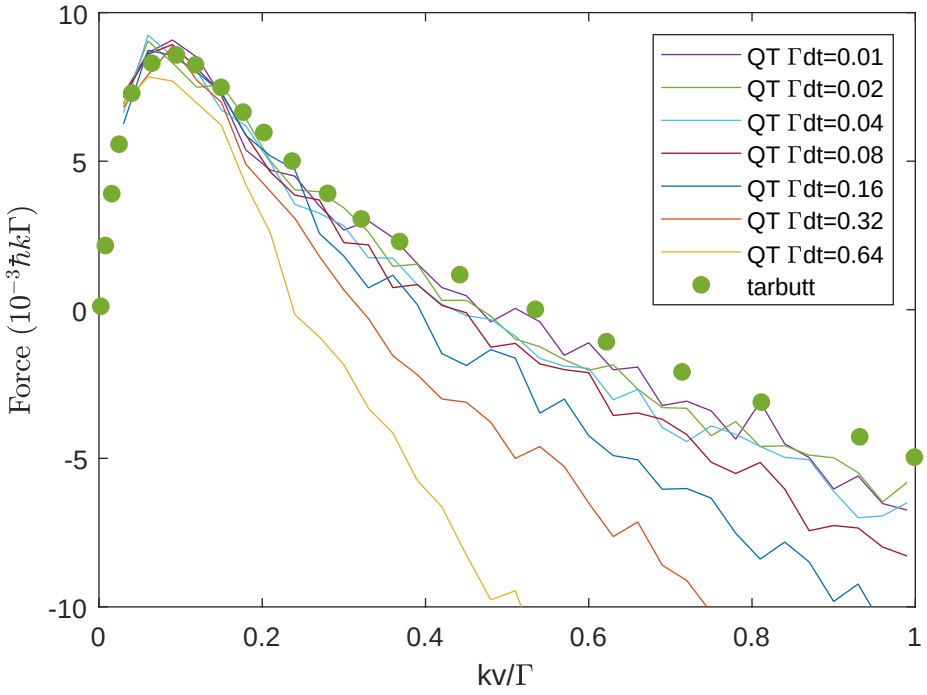

Figure 1.2: $\vec{F} \cdot \vec{v}/|v|$ vs $|v|$ for various dt ($\delta = -2.5$, $\Omega = 1/\sqrt{2}$). We observe good agreement for low dt. As dt increases, the curves begin to diverge at high v.

products of the wavefunctions obtained in steps 2 and 3

After step 1 we have, for the 4 X states:

- $|F = 2; J = 3/2\rangle$
- $0.888|F = 1; J = 3/2\rangle + 0.4598|F = 1; J = 1/2\rangle$
- $|F = 0; J = 1/2\rangle$
- $-0.4598|F = 1; J = 3/2\rangle + 0.888|F = 1; J = 1/2\rangle$

For step 2, the formula cited in John Barry's thesis is:

$$|\Lambda; N, S, J\rangle = \sum_{\Omega=-1/2}^{1/2} \sum_{\Sigma=-1/2}^{1/2} (-1)^{J+\Omega} \sqrt{2N+1} \begin{pmatrix} S & N & J \\ \Sigma & \Lambda & -\Omega \end{pmatrix} |\Lambda, S, \Sigma, \Omega, J\rangle \tag{1.6}$$

Applying this to the X states derived in step 1 yields the following for the expression of X states (currently ignoring zeeman substructure) in the Hunds (a) basis:

- $\frac{1}{\sqrt{2}} [|F = 2; J = 3/2, \Omega = 1/2, \Sigma = 1/2\rangle + |F = 2; J = 3/2, \Omega = -1/2, \Sigma = -1/2\rangle]$

- $\frac{1}{\sqrt{2}}\left[0.888|F=1;J=3/2,\Omega=1/2,\Sigma=1/2\rangle+0.888|F=1;J=3/2,\Omega=-1/2,\Sigma=-1/2\rangle\right]$
  $+\frac{1}{\sqrt{2}}\left[-0.4598|F=1;J=1/2,\Omega=1/2,\Sigma=1/2\rangle+0.4598|F=1;J=1/2,\Omega=-1/2,\Sigma=-1/2\rangle\right]$
- $\frac{1}{\sqrt{2}}\left[-|F=0;J=1/2,\Omega=1/2,\Sigma=1/2\rangle+|F=0;J=1/2,\Omega=-1/2,\Sigma=-1/2\rangle\right]$
- $\frac{1}{\sqrt{2}}\left[-0.4598|F=1;J=3/2,\Omega=1/2,\Sigma=1/2\rangle-0.4598|F=1;J=3/2,\Omega=-1/2,\Sigma=-1/2\rangle\right]$
  $+\frac{1}{\sqrt{2}}\left[-0.888|F=1;J=1/2,\Omega=1/2,\Sigma=1/2\rangle+0.888|F=1;J=1/2,\Omega=-1/2,\Sigma=-1/2\rangle\right]$

In step 3, we write the positive parity A states using Eq 6.234 of Brown and Carrington as:

- $\frac{1}{\sqrt{2}}\left[|F'=1;J'=1/2,\Omega'=1/2,\Sigma'=-1/2\rangle+|F=1;J=1/2,\Omega'=-1/2,\Sigma'=1/2\rangle\right]$
- $\frac{1}{\sqrt{2}}\left[|F'=0;J'=1/2,\Omega'=1/2,\Sigma'=-1/2\rangle+|F=0;J=1/2,\Omega'=-1/2,\Sigma'=1/2\rangle\right]$

Finally, we must use angular momentum addition rules to obtain the correct CG coefficients. First, we need to know what the inner product of two given eigenstates coupled by some light field is (e.g., what $\langle\Omega,\Sigma,J,F,m_F|T^1_p|\Omega',\Sigma',J',F',m'_F\rangle$ where T^1_p is the electric dipole operator written in spherical tensor notation and p refers to the polarization (0 for π, +1 for σ^+, -1 for σ^{-1}, etc.). From (Tarbutt, Norrgard), we determine:

$$C(F',F,m'_F,m_F,\Omega',\Omega,\Sigma',\Sigma,p,J',J,I)=m_1(F',F,m'_F,m_F,p)m_2(F',F,J',J,I)m_3(J',J,\Omega',\Omega)\delta_{\Sigma,\Sigma'} \tag{1.7}$$

where

$$m_1(F',F,m'_F,m_F,p)=(-1)^{F'-m'_F}\begin{pmatrix}F' & m'_F & 1\\ p & F & m_F\end{pmatrix} \tag{1.8}$$

$$m_2(F',F,J',J,I)=(-1)^{F'+J+1+I}\sqrt{(2F'+1)(2F+1)}\begin{Bmatrix}J' & F' & I\\ F & J & 1\end{Bmatrix} \tag{1.9}$$

(spectator theorem used in m_2)

$$m_3(J',J,\Omega',\Omega)=\sum_{q=-1}^{1}(-1)^{J'-\Omega'}\sqrt{(2J'+1)(2J+1)}\begin{pmatrix}J' & 1 & J\\ -\Omega' & q & \Omega\end{pmatrix} \tag{1.10}$$

Finally, we can now calculate CG coeffs for electric dipole coupling between X and A states. For example, to calculate the CG coefficient for the coupling of $|F=2,m_F=2\rangle$ to $|F'=1,m_F=1\rangle$ using σ^- polarized light, we must calculate:

$$\frac{1}{2}\left[C(1,2,1,2,1/2,-1/2,1/2,1/2,-1,1/2,3/2,1/2)+C(1,2,1,2,-1/2,1/2,-1/2,-1/2,-1,1/2,3/2,1/2)\right] \tag{1.11}$$

where I have already evaluated the inner product components where $\Sigma\neq\Sigma'$ to be zero. When I evaluate this, I obtain a coefficient of $1/\sqrt{6}$. Below I include

			$F'=0$		$F'=1$	
J	F	m_F	$m'_F=0$	$m'_F=-1$	$m'_F=0$	$m'_F=1$
3/2	2	-2	0	$1/\sqrt{6}$	0	0
3/2	2	-1	0	$-1/2\sqrt{3}$	$1/2\sqrt{3}$	0
3/2	2	0	0	$1/6$	$-1/3$	$1/6$
3/2	2	1	0	0	$1/2\sqrt{3}$	$-1/2\sqrt{3}$
3/2	2	2	0	0	0	$1/\sqrt{6}$
3/2	1	-1	0.5128	0.0688	0.0688	0
3/2	1	0	-0.5128	-0.0688	0	0.0688
3/2	1	1	0.5128	0	-0.0688	-0.0688
1/2	0	0	0	$\sqrt{2}/3$	$\sqrt{2}/3$	$\sqrt{2}/3$
1/2	1	-1	-0.2653	0.4952	0.4952	0
1/2	1	0	0.2653	-0.4952	0	0.4952
1/2	1	1	-0.2653	0	-0.4952	-0.4952

a table of all CG coefficients (which in the future I will write as $CG_{J,F,m,F',m'}$) (squaring the terms in this table **does not** give a result equivalent to the branching ratios shown in Table 2.15 of John Barry's thesis. I've discussed this elsewhere, but there is an error in his calculation where the J-mixing terms are not taken into account correctly).

Following (simul laser cooling paper), the atom-light hamiltonian for SrF addressed by one laser (note: laser detuning δ will always be defined relative to the $|F=1\downarrow\rangle \rightarrow A^2\Pi_{1/2}$):

$$H = H_E + H_{coup} \tag{1.12}$$

where

$$H_E = \sum_{F,J,m} |F,J,m\rangle \hbar\Delta_{F,J}\langle F,J,m| - \sum_{F',m'} |F',m'\rangle\hbar\delta\langle F',m'| \tag{1.13}$$

$\Delta_{1,1/2}=0$, $\Delta_{0,1/2}=7.5\Gamma$, $\Delta_{1,3/2}=19.6\Gamma$, $\Delta_{2,3/2}=25.9\Gamma$, and

$$\begin{aligned} H_{coup} =& \frac{\hbar\Omega}{2}\Big[c_{\sigma^+}\sum_{J,F,m,F'} CG_{J,F,m,F',m'=m+1}|J',F',m+1\rangle\langle J,F,m| \\ &+ c_{\pi}\sum_{J,F,m,F'} CG_{J,F,m,F',m'=m}|J',F',m\rangle\langle J,F,m| \\ &+ c_{\sigma^-}\sum_{J,F,m,F'} CG_{J,F,m,F',m'=m-1}|J',F',m-1\rangle\langle J,F,m|\Big] \end{aligned} \tag{1.14}$$

The addition of other lasers with Rabi frequency Ω_L and detuning δ_L (detuning is with respect to the "first" laser, so $\delta_L = \nu_L - \nu_0$ where ν_L is the frequency of the additional laser and ν_0 is the frequency of the "original laser") is accomplished by adding terms of the form:

$$
\begin{aligned}
H_{coupAdd} =& \frac{\hbar\Omega_L \exp\left[i\hbar\delta_L t_a\right]}{2}\Big[c_{\sigma^+}\sum_{J,F,m,F'} CG_{J,F,m,F',m'=m+1}|J',F',m+1\rangle\langle J,F,m| \\
&+ c_\pi \sum_{J,F,m,F'} CG_{J,F,m,F',m'=m}|J',F',m\rangle\langle J,F,m| \\
&+ c_{\sigma^-}\sum_{J,F,m,F'} CG_{J,F,m,F',m'=m-1}|J',F',m-1\rangle\langle J,F,m|\Big]
\end{aligned}
\tag{1.15}
$$

Handling the time component takes a little bit of care. One must track the time over which each particle has NOT jumped (e.g., if it has been $t = 5\Gamma^{-1}$ since particle a has jumped, then $t_a = 5$ even if the simulation has been running for $t_{sim} > t_a$. If particle a jumps during a given timestep, then on the next timestep t_a is reset to 0).

Bibliography

[1] M. Lukin, *Modern Atomic and Optical Physics II Textbook*,

[2] P. D. Lett, W. D. Phillips, S. L. Rolston, C. E. Tanner, R. N. Watts, and C. I. Westbrook, *Optical Molasses*, Journal of the Optical Society of America B, 6, 11, 2084 (1989)

[3] J. A. Devlin and M. R. Tarbutt, *Three-dimensional Doppler, polarization-gradient, and magneto-optical forces for atoms and molecules with dark states* , New Journal of Physics, 18, 123017, (2016)

[4] J. Dalibard, Y. Castin, and K. Molmer, *Wave-Function Approach to Dissipative Processes in Quantum Optics* , Phys. Rev. Lett., (1992)

[5] H. J. Carmichael, *Quantum Trajectory Theory for Cascaded Open Systems*, Phys. Rev. Lett., (1993)

[6] J. Dalibard and C. Cohen-Tannoudji, *Laser cooling below the Doppler limit by polarization gradients: simple theoretical models*, J. Opt. Soc. Am. B, (1989)